SEPTEMBER 1, 2000

Environmental Science & Technology

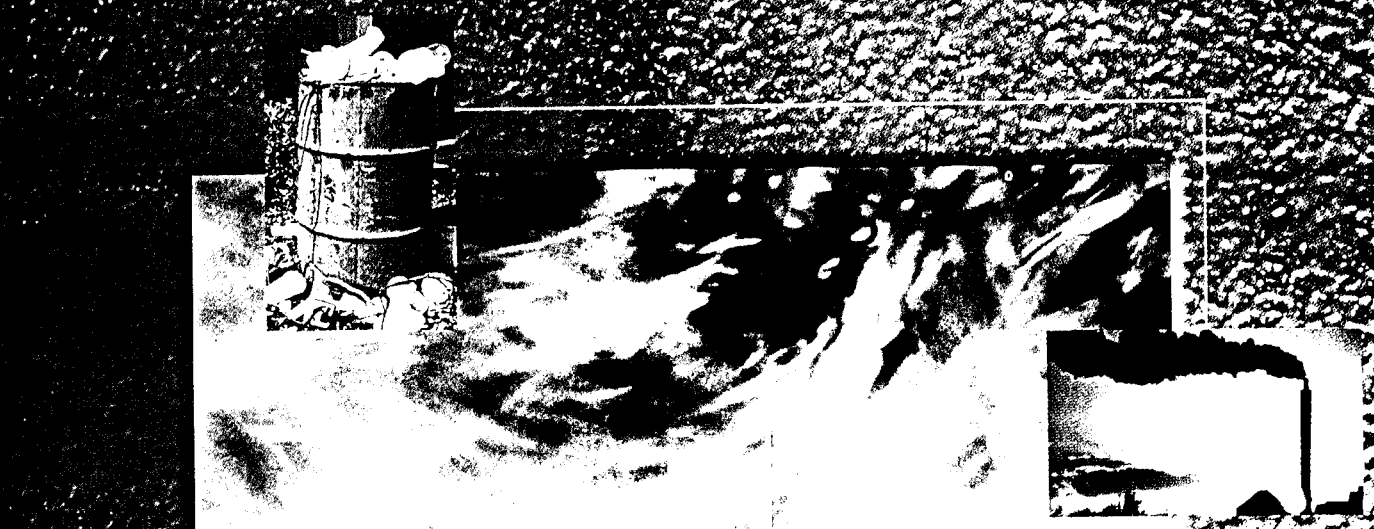

The Health Impacts of INCINERATION

PUBLISHED BY THE AMERICAN CHEMICAL SOCIETY

Environ Sci Technol 2000, 34, 3737–3741

Experimental Study of Uranyl Adsorption onto *Bacillus subtilis*

DAVID A FOWLE,* JEREMY B FEIN, AND AARON M MARTIN

Department of Civil Engineering and Geological Sciences, University of Notre Dame, Notre Dame, Indiana 46556

Uranyl adsorption onto the Gram-positive soil bacterium *Bacillus subtilis* was measured using batch experiments in 0.1 M $NaClO_4$ as a function of pH, time, and solid solute ratio at 25 °C. The experimental data were interpreted using a surface complexation approach. The experimental measurements constrain the stoichiometry and thermodynamic stabilities of the important uranyl-surface complexes. The U adsorption data require two separate adsorption reactions, with the uranyl ion forming surface complexes with the neutral phosphate functional groups and the deprotonated carboxyl functional groups of the bacterial cell wall: $R-POH^0 + UO_2^{2+} \leftrightarrow R-POH-UO_2^{2+}$ (log $K = 11.8 \pm 0.2$) and $R-COO^- + UO_2^{2+} \leftrightarrow R-COO-UO_2^+$ (log $K = 5.4 \pm 0.2$). These new stability constants, in conjunction with other experimental and predicted stability constants, may be incorporated in surface complexation models to determine the mobility and fate of U in bacteria-bearing water–rock systems.

Introduction

The release and subsequent transport of uranium and other radionuclides in near-surface geological systems has focused research on developing accurate and versatile predictive tools for determining the fate of uranium in water–rock systems. The mobility of uranium in low-temperature water–rock systems is controlled by the solubility of secondary uranium mineral phases (*1*, *2*), the sorption of uranium to inorganic and biological substrates (*3–5*), the redox chemistry of uranium (*6–9*), and the tendency of uranium to form stable aqueous complexes (*6*). Significant efforts have been made to develop a thermodynamic database that can accurately describe the aqueous geochemistry of uranium in these systems (*6*, *10*, *11*).

Cell densities of 10^5–10^9 cells/g of soil or aquifer material have been reported, potentially representing a significant proportion of reactive surface area exposed to fluid (*12*, *13*). If not attached to the aquifer substrate but entrained in the fluid flow, the colloidal size of bacterial cells may lead to enhanced transport of aqueous metal cation contaminants (such as UO_2^{2+}) through adsorption reactions (*14*). However, without a theoretical framework to quantify the interactions between microorganisms and uranium (and other radionuclides), it remains difficult to incorporate uranium–bacteria interactions into current contaminant transport models.

Bacterial sorption may affect the fate of uranium in many near-surface environments. Laboratory and field studies have demonstrated that microbes have the ability to facilitate the removal of uranium from the aqueous phase through the sorption of U(VI) to bacterial cell walls (*5*, *15*), through the biological reduction of U(VI) (*7–9*), and through enzymatic production or nucleation of U mineral precipitates (*16*, *17*). The high affinity of bacteria for U and other radionuclides has led to a number a studies that measure the binding capacity of a particular microorganism under a unique set of experimental conditions (for a thorough review of these studies, see ref *5*). Many researchers have investigated uranium sorption onto microbial cell wall surfaces. For example, studies by Friis and Myers-Keith (*18*) and Cotoras et al. (*19*) quantified the ability of *Streptomyces longwoodensis* and *Micrococcus* to bind U through the use of system-specific binding constants or chemical equilibria modeling. In each of these studies, however, a site-specific surface complexation approach was not invoked, therefore, the experimental results cannot be used to estimate the effect that changes in pH or other aqueous chemistry would have on adsorption. Each of these studies has helped to demonstrate that bacteria are likely to play a significant role in the transport and fate of U in the subsurface. However, none of them enable quantitative predictions of the extent of U adsorption onto bacterial cell walls under conditions not directly studied in the laboratory. Toward this end, we investigated the sorption of U by the Gram-positive soil bacterium *Bacillus subtilis*. This bacterium was selected for this study because its cell wall properties have been well-characterized through microbiological and biochemical assays (*20*, *21*) and its surface and acid/base properties have been previously described by our lab (*22–24*). Utilizing *B. subtilis* in our experiments is also an environmentally relevant choice because this species is a common soil microorganism that has been isolated from uranium mine settings and has demonstrated a strong ability to bind U (*25*).

Our objective is to test whether the site-specific surface complexation model (SCM) of Fein et al. (*22*) can be used to quantify U adsorption onto *B. subtilis*. The SCM for *B. subtilis* describes specific adsorption reactions between the functional groups of the bacterial cell wall and the species in solution through mass action laws that are governed by thermodynamic stability constants. The bacterial surface deprotonation reactions for the carboxyl, phosphate, and hydroxyl functional groups are characterized by the following reactions (*22*):

$$R-COO-H^0 \leftrightarrow R-COO^- + H^+ \quad pK_a = 4.82 \qquad (1)$$

$$R-PO-H^0 \leftrightarrow R-PO^- + H^+ \quad pK_a = 6.9 \qquad (2)$$

$$R-O-H^0 \leftrightarrow R-O^- + H^+ \quad pK_a = 9.4 \qquad (3)$$

where R represents the bacterium to which each functional group is attached. The site densities and surface area utilized for this model have been determined by Fein et al. (*22*). Deprotonation of the cell wall functional groups creates negatively charged surface sites for metal adsorption according to the general reaction (written for a generic surface functional group, A)

$$M^{m+} + R-A^- \leftrightarrow R-A-M^{(m-1)} \qquad (4)$$

The deprotonation also leads to the development of a negative electrical potential associated with the bacterial cell wall. This potential in turn affects the interactions of ions

* Corresponding author present address: Geology and Geophysics, University of Wisconsin–Madison, 1215 W. Dayton St., Madison, WI 53706; telephone: (608)262-4983; fax: (608)262-0693; e-mail: fowle@geology.wisc.edu.

10.1021/es991356h CCC: $19.00
Published on Web 07/25/2000

with the bacterial surface sites We can account for these effects on surface acidity constants and metal stability constants through the following relationship

$$K = K_{\text{intrinsic}} e^{(-\Delta Z F \varphi_0 / RT)} \quad (5)$$

where ΔZ is the change in the charge of the surface species for the reaction under consideration, F and R are Faraday's constant and the gas constant, respectively; T is absolute temperature, $K_{\text{intrinsic}}$ represents the equilibrium constant referenced to zero surface charge, and φ_0 is the electric field potential of the bacterial surface (*26*) We relate the surface electrical potential to surface charge (σ) by a constant capacitance double-layer model

$$C = \frac{\sigma}{\psi} \quad (6)$$

where C is the capacitance of the *B subtilis* surface (8 0 F/m^2) (*19*) With this approach, equilibrium constant values can be used to quantitatively predict the extent of proton and metal adsorption onto specific bacterial surface sites over a wide range of pH, metal concentration, and surface site concentration conditions (*22, 23, 27*) The approach can also successfully account for competitive adsorption (metal cations) effects (*28*), for the competition between aqueous organic acids, and for the bacterial surface for available metal cations (*29*)

In this study, we document the adsorption of U onto the Gram-positive bacterium *B subtilis*, and we invoke a site-specific SCM to model these interactions This study provides insights in the pH dependence, reversibility, and kinetics of U−*B subtilis* adsorption reactions

Experimental Procedures

The bacterial species *B subtilis* was prepared and cultured following the procedure outlined in Fein et al (*22*) and Fowle and Fein (*24*) Integrity of the cell walls after the wash procedure was monitored using microscopy and Molecular Probes−LIVE/DEAD *Bac*Light bacterial viability kit All solutions in this study were prepared with distilled, deionized (18 MΩ) water Prior to each experiment, the bacteria were pelleted by centrifugation at 7500 rpm for 60 min The mass of the pellet was measured in order to determine the concentration of surface functional groups in each experiment Note that the weight of bacteria used in each experiment is not reported as a dried weight but as a weight after centrifugation

The sorption of U by *B subtilis* was studied in 0 1 M $NaClO_4$ electrolyte solutions Batch experiments were conducted at 25 ± 1 °C as a function of pH, solid/solute ratio, and equilibration time Bacteria were suspended in 0 1 M $NaClO_4$ electrolyte, and 1000 ppm aqueous U standard was added to the bacteria−electrolyte solution to create a homogeneous parent solution of known bacterial (0 5, 1 0, or 1 5 g/L) and U concentrations (0 084 mM) Aliquots of the parent solution were transferred to the reaction vessels (acid-washed polypropylene), and the pH of the suspension in each vessel was adjusted to the desired pH value using small volumes (less than 1% of total experimental volume) of standardized HNO_3 or NaOH The pH interval of 1 5−5 0 was chosen to focus the study on UO_2^{2+} adsorption At higher pH values, hydroxyl and carbonate complexation of UO_2^{2+} complicates the aqueous and surface U speciation (the positively charged hydrolysis products and carbonate complexes may adsorb) and was beyond the scope of this initial study The reaction vessels were placed on a rotating rack that provided gentle (10 rpm) end-over-end agitation The equilibrium pH was recorded, and the suspension was filtered through a 0 1-μm nylon filter The filtrate was acidified and analyzed for U content by ICP-AES (with an analytical uncertainty of ±2%) The bacteria do not lyse, sporolate, or multiply during our experiments, therefore, cell concentrations or surface area changes do not affect our results Control experiments followed the experimental procedure without the presence of bacteria

Desorption experiments were conducted to determine the reversibility of U−bacteria adsorption reactions A homogeneous parent solution of bacteria + U + electrolyte was adjusted to pH 5 0 (a pH at which nearly all of the U was adsorbed onto the bacteria) as described above Aliquots from this parent solution were taken and adjusted to sequentially lower pH values (4 8−1 8) after 2 h of adsorption contact time The reaction vessels equilibrated at the new pH values for 2 h and were sampled for U content as described above

Results and Discussion

The cell walls of *B subtilis* display a strong affinity for U (Figure 1) The control experiments revealed a minor pH-dependent systematic loss (1−10%) of U from pH 1 5 to pH 5 0, likely caused either by adsorption of UO_2^{2+} onto the reaction vessels or by the formation of a uranium precipitate All of our data were adjusted by fitting a linear regression to the control data to correct for this loss The adjusted data is depicted in Figures 1 and 3 The concentration of U bound to the bacterium is strongly dependent on the solid solute ratio and the solution pH Adsorption increases with increasing pH and solid solute ratio, presumably due to the deprotonation of cell wall functional groups and the increasing number of surface reactive sites The adsorption of U reaches equilibrium within 30 min and remains invariant through at least 24 h A maximum U adsorption of 90% was observed at pH 4 9 (1 5 g of bacteria/L), and the minimum adsorption of U of 12% was observed at pH 1 7 (0 5 g of bacteria/L) Remarkably, up to nearly 60% of the aqueous U (1 5 g of bacteria/L) was adsorbed at solution pH values less than 2, conditions at which virtually all surface sites are fully protonated and neutrally charged This is in marked contrast to the adsorption behavior of other cations onto *B subtilis*, which exhibit only small or negligible adsorption under such low pH conditions (*22, 23, 28*) Desorption experiments (Figure 1c), conducted at 1 5 g of bacteria/L, are in excellent agreement with adsorption experiments, indicating that the adsorption of U is both rapid and reversible Furthermore, the rapid kinetics and reversibility of U binding in conjunction with TEM images of *B subtilis*, which demonstrate that U binds to the outside of the cell (*30*), strongly suggest that the loss of U from the aqueous phase in these undersatuated systems is through adsorption to the organic functional groups of the bacterial cell wall

The experimental data were used to calculate stability constants for the U−functional group adsorption reactions We use the program FITEQL 3 1 (*31*) to compare models involving different U adsorption reaction stoichiometries and to determine the model that most accurately describes our data Figure 2 illustrates the aqueous speciation of U under the experimental conditions Because of the predominance of UO_2^{2+} over the pH range studied, it is most likely that UO_2^{2+} is responsible for the U uptake under the experimental conditions We choose to model the system using the following reaction stoichiometry

$$UO_2^{2+} + R{-}AH_x^{(x-1)} \leftrightarrows R{-}AH_x{-}UO_2^{(1+x)} \quad (7)$$

where A represents either a carboxyl, a phosphate, or a hydroxyl surface functional group, and x can equal either 0 or 1 We test all possible adsorption site stoichiometries and

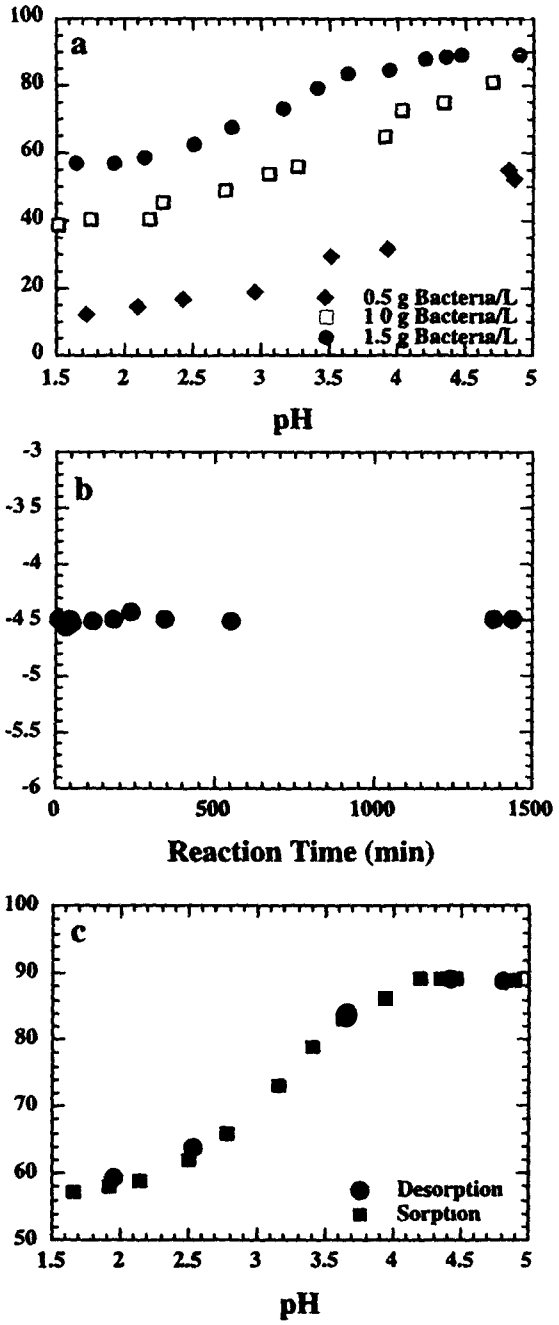

FIGURE 1 (a) Percent adsorption of U by *B subtilis* as a function of pH Experiments were conducted in 0.1 $NaClO_4$ with $10^{-4.00}$ M U and with 0.5, 1.0, or 1.5 g of bacteria/L. (b) Percent adsorption of U by *B subtilis* as a function of time. Experiments were conducted in 0.1 $NaClO_4$ at pH 3.0 with $10^{-4.00}$ M U and with 0.5 g of bacteria/L. (c) The percent of total U associated with the bacterial surface after adsorption (squares) and desorption (circles) as a function of pH in 0.1 M $NaClO_4$ with a total system concentration of $10^{-4.00}$ M U and a bacterial concentration of 1.5 g/L. Desorption began after a 2-h period of adsorption at pH 5.0. pH was then lowered to between 2 and 5.

solve for stability constants for each proposed stoichiometry, as defined by

$$K_{(7)} = \frac{[\text{R}-\text{AH}_x-\text{UO}_2^{(1+x)}]}{a_{\text{UO}_2^{2+}}[\text{R}-\text{AH}_x^{(x-1)}]} \qquad (8)$$

where a represents aqueous activity and the brackets represent surface site concentrations in moles per kilogram of solution. The calculation of the stability constants for the surface complexation reactions uses the equilibrium constants from Fein et al. (*22*) for the acid/base properties of *B subtilis* and those of Wolery (*32*) for aqueous reactions in the $Na-ClO_4-NO_3-H_2O$ system. The values and sources of the formation constants for the various uranium aqueous species used in this study are listed in Table 1.

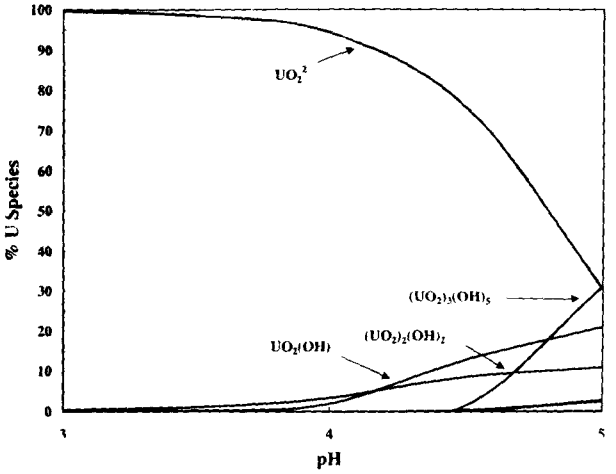

FIGURE 2. Calculated aqueous speciation of U at 25 °C and 1 bar with aqueous concentrations of $10^{-4.00}$ M U, $10^{-3.5}$ M CO_2(aq), and 0.1 M $NaClO_4$ as function of pH

TABLE 1 U(VI) Aqueous Phase Reactions

reaction	log K (I = 0.0, 25 °C)
$UO_2^{2+} + H_2O \rightleftharpoons UO_2OH^+ + H^+$	−5.2
$UO_2^{2+} + 2H_2O \rightleftharpoons UO_2(OH)_2 + 2H^+$	−12.0
$UO_2^{2+} + 3H_2O \rightleftharpoons UO_2(OH)_3^- + 3H^+$	−19.2
$2UO_2^{2+} + 2H_2O \rightleftharpoons (UO_2)_2(OH)_2^{2+} + 2H^+$	−5.62[a]
$3UO_2^{2+} + 5H_2O \rightleftharpoons (UO_2)_3(OH)_5^+ + 5H^+$	−15.55
$3UO_2^{2+} + 7H_2O \rightleftharpoons (UO_2)_3(OH)_7^- + 7H^+$	−31.0
$4UO_2^{2+} + 7H_2O \rightleftharpoons (UO_2)_4(OH)_7^+ + 7H^+$	−21.9
$UO_2^{2+} + CO_3^{2-} \rightleftharpoons UO_2CO_3^0$	9.7
$UO_2^{2+} + 2CO_3^{2-} \rightleftharpoons UO_2(CO_3)_2^{2-}$	17.0
$UO_2^{2+} + 3CO_3^{2-} \rightleftharpoons UO_2(CO_3)_3^{4-}$	23.63
$2UO_2^{2+} + CO_3^{2-} + 3OH^- \rightleftharpoons (UO_2)_2CO_3(OH)_3^-$	40.82[b]

[a] From ref *11*. [b] From ref *38*. All other stability constants from ref *6*.

The misfit of each model is quantified using the $V(Y)$ variance function in FITEQL.

$$V(Y) = \frac{\sum\left(\frac{Y_{\text{calc}} - Y_{\text{exp}}}{s_{\text{exp}}}\right)^2}{n_p n_{\text{II}} - n_u} \qquad (9)$$

where Y_{calc} and Y_{exp} are the calculated and the experimental data, s_{exp} is the error associated with the experimental data (default FITEQL 3.1 value), n_p is the number of data, n_{II} is the number of group II components (total and free concentrations are known), n_u is the number of adjustable parameters, and $V(Y)$ is the variance in Y. The $V(Y)$ value provides a quantitative measure of the goodness of fit of each model, and we use this parameter to determine the best-fitting model.

Adsorption of UO_2^{2+} onto deprotonated carboxyl sites is the only mechanism that can reasonably explain the pH dependence of adsorption that we observed between approximately pH 2.5 and pH 5.0. Models involving adsorption of UO_2^{2+} onto deprotonated phosphate or hydroxyl sites offer poor fits to the pH-dependent adsorption behavior

TABLE 2 Comparison of UO_2–*B. subtilis* Adsorption Models

bacterial conc	model[a]	log *K*[b]	*V*(*Y*)[c]
1 5 g of bacteria/L	R–COOH–UO_2^{2+}	9 04	3 823
	R–COO–UO_2^{+}	5 71	
	R–PO_4H–UO_2^{2+}	11 88	1 994
	R–COO–UO_2^{+}	5 432	
	R–OH–UO_2^{2+}	14 08	2 334
	R–COO–UO_2^{+}	5 50	
1 0 g of bacteria/L	R–COOH–UO_2^{2+}	8 93	4 31
	R–COO–UO_2^{+}	5 58	
	R–PO_4H–UO_2^{2+}	11 76	6 186
	R–COO–UO_2^{+}	5 36	
	R–OH–UO_2^{2+}	DNC[e]	DNC[e]
	R–COO–UO_2^{+}		
0 5 g of bacteria/L	R–COOH–UO_2^{2+}	8 36	24 97
	R–COO–UO_2^{+}	5 53	
	R–PO_4H–UO_2^{2+}	11 83	27 88
	R–COO–UO_2^{+}	5 303	
	R–OH–UO_2^{2+}	13 23	28 38
	R–COO–UO_2^{+}	5 439	
best-fitting model[d]	R–PO_4H–UO_2^{2+}	11 8 ± 0 2	
	R–COO–UO_2^{+}	5 4 ± 0 2	

[a] Models consider formation of surface complexes due to adsorption of UO_2^{2+} onto the carboxyl, phosphate, and hydroxyl surface sites [b] Log *K* values are referenced to zero surface charge at 25 °C [c] Variance as calculated by FITEQL [d] Choice of best fitting model is based upon fit of weighted average log *K* values and overall variance as calculated by FITEQL. [e] DNC, did not converge

In addition, models that included multi-dentate uranyl surface species resulted in a poor fit to the experimental data and are not considered further However, the pH-dependent adsorption behavior is inconsistent with the adsorption observed under low pH conditions, where we observe pH-independent adsorption, the extent of which appears to be directly related to the amount of bacteria in the system This pH-independent behavior requires an adsorption species whose concentration does not vary over at least the pH range of 1 5–2 5 Under these conditions, each surface functional group type is virtually fully protonated, with negligible changes in concentration over this pH interval Therefore, we test each possible combination, with each tested model coupling UO_2^{2+} adsorption onto deprotonated carboxyl sites with adsorption of UO_2^{2+} onto either a protonated carboxyl, phosphate, or hydroxyl site The results of these calculations, for each model and bacteria concentration, are compiled in Table 2

The results in Table 2 demonstrate that the best-fitting model is the one involving low pH adsorption onto protonated phosphate sites Several lines of evidence support this conclusion (i) for each set of bacterial concentration data, this model yields a good fit to the data, as demonstrated by low $V(Y)$ values, (ii) this model yields the smallest variations in the calculated log *K* values for each surface complex between bacterial concentration data sets, (iii) independent ^{31}P NMR measurements have demonstrated that UO_2^{2+} binding to phosphate sites of *Mycobacterium smegmatis* occurs at pH values as low as 1 0 (*33*), and (iv) metal complexes with protonated phosphate ligands are well documented (*34, 35*), whereas protonated metal–carboxylate complexes are unlikely to possess the large stability constants constrained in this study Each data set yields a best-fitting stability constant value for the two surface species, and we calculate the weighted average stability constant values from the three data sets, yielding a single value for each equilibrium constant that together provide the best-fitting model to all of the data For UO_2^{2+} adsorption onto protonated phosphate sites ($K_{(7)}$, with A representing a phosphate site, and $x = 1$), the best-fitting value of log *K* is 11 8 ± 0 2 For UO_2^{2+} adsorption onto deprotonated carboxyl sites ($K_{(7)}$, with A representing a carboxyl site, and $x = 0$), log *K* is 5 4 ± 0 2

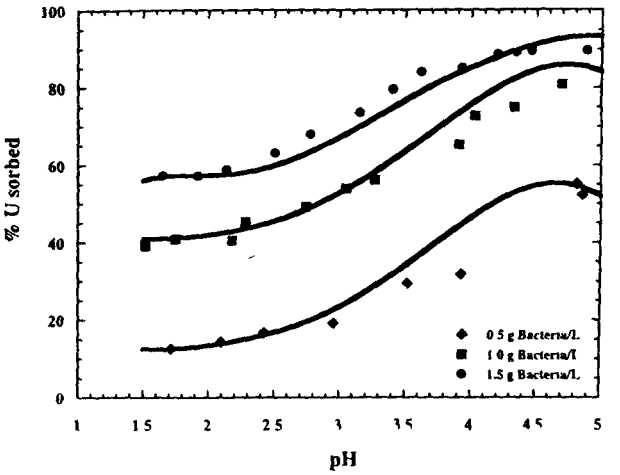

FIGURE 3 U adsorption onto *B. subtilis* as a function of pH The curves represent the best-fitting surface complexation model for each bacterial concentration, calculated using the weighted average values of the equilibrium constants of the adsorption reactions

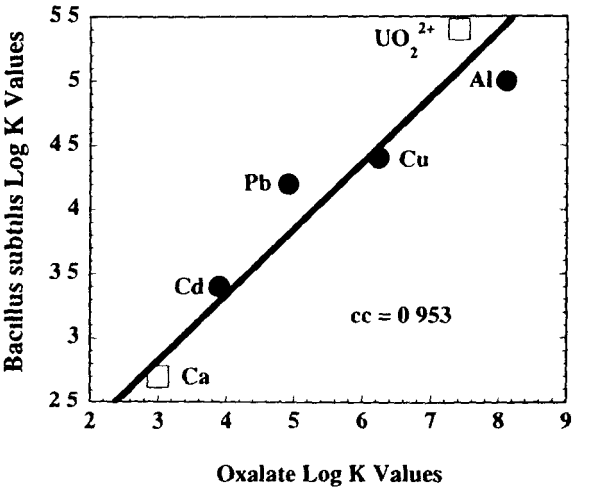

FIGURE 4 Correlation diagram relating metal–carboxyl site (on *B. subtilis* cell wall) log stability constants to the aqueous metal–oxalate log stability constants The linear correlation coefficient is shown for the relationship

Figure 3 depicts the experimental data and model predictions for the adsorption of U onto *B. subtilis* at the three different bacteria concentrations Each curve is in excellent agreement with its corresponding data from pH 1 5 to pH 2 0 Above pH 2 0, the experimental data are slightly overpredicted by the model for the 1 5 g of bacteria/L system and underpredicted for the other bacterial concentrations However, these discrepancies are minor and within the uncertainties for the stability constants Therefore, we conclude that these two adsorption stoichiometries, with the two calculated stability constant values, can accurately account for both the pH dependence and the solid solute ratio dependences of adsorption

Although only a limited number of metal–bacteria adsorption reactions have been studied to date, recent work (*22, 23*) suggests that metal–carboxyl stability constants can be estimated with reasonable accuracy, using a linear free energy approach (*36*) We can use the results of this study to place additional constraints on these relationships Figure 4 shows the relationship between aqueous metal–oxalate stability constants and those determined for metal adsorption onto deprotonated carboxyl sites on *B. subtilis* The data are from Fein et al (*22*) for Al, Pb, Cd, and Cu, from Fowle and Fein (*28*) for Ca, and from this study for UO_2^{2+} Fein et al

(22) determined a similar correlation between *B subtilis* stability constants and those involving iron However, an accurate aqueous UO_2^{2+}–iron stability constant value has not been measured, and so we cannot further constrain this relationship with our new data Stability constants used for metal–oxalate complexation are those described in Martell and Smith (*34, 35*) The values were adjusted (if necessary) to zero ionic strength using the Debye–Hückel equation with parameters from Hegleson et al (*37*) Figure 4 illustrates an excellent correlation between aqueous and bacterial surface metal–organic complexation, indicating that metal–bacteria surface carboxyl complexes may include partial bonding contributions from more than one carboxyl oxygen considering the strong correlation with metal chelating ligand oxalate The linear correlation coefficient is 0 953, a high value especially given the uncertainties in the metal–organic stability constants, the metal–carboxyl stability constants, and uncertainties in applying the Debye–Hückel equation to relatively high ionic strengths and to di- and especially trivalent ions This striking relationship appears to be robust, and the inclusion of the new Ca and UO_2^{2+} data enables us to extend the range of the linear free energy relationship by an order of magnitude Metal–bacteria adsorption behavior can now be estimated for a much wider range of metals

Bacterial adsorption may significantly affect the distribution and, hence, mobility of uranium in groundwater systems Our results offer a first step toward quantifying the speciation of U in bacteria-bearing systems The study of metal–bacteria adsorption is in its infancy, and many more interactions must be quantified before surface complexation models of realistic systems are possible However, it is the vast range of systems that are of geologic and environmental interest that makes the surface complexation approach so powerful To apply a surface complexation approach, a large number of isolated stability constants must be determined, either by direct measurement or by estimation techniques, but there is no other technique that yields quantitative estimations of metal distributions over a broad range of near-surface geological conditions

Acknowledgments

Acknowledgment is made to the donors of the Petroleum Research Fund, administered by the American Chemical Society, for partial support of this research This work was also supported by National Science Foundation Grant EAR-9905704 The authors thank Y Suzuki for his help in identifying some pertinent literature A M M was supported by a National Science Foundation (Research Experience for Undergraduates) grant The manuscript benefited greatly from constructive journal reviews by three anonymous referees

Literature Cited

(1) Burns, P C , Ewing, R. C , Miller, M L. *J Nucl. Mater* **1996** *245* 1
(2) Murakami, T , Ohnuki, T , Isobe, H , Sato, T *Am. Mineral* **1997** *82*, 888
(3) Waite, T D , Davis, J A , Payne, T E , Waychunas, G A Xu N *Geochim. Cosmochim Acta* **1994**, *58*, 5465
(4) Turner, G D , Zachara, J M , McKinley, J P , Smith, S C *Geochim Cosmochim Acta* **1996**, *60*, 3399
(5) Suzuki, Y , Banfield, J F , Geomicrbiology of Uranium In *Uranium Mineralogy, Geochemistry and the Environment*; Burns, P C , Finch, R , Eds , Reviews in Mineralogy 38, Mineralogical Society of America Washington, DC, 1999 p 393
(6) Grenthe, I , Fuger J , Konings, R J M , Lemire, R J Muler, A. B , Nguyen Trung, C , Wanner, H *Chemical thermodynamics of uranium* Chemical Thermodynamic Series, Elsevier Amsterdam, 1992
(7) Lovely, D R , Phillips, E J P Gorby, Y A , Landa, E R *Nature* **1991** *350* 413
(8) Lovely D R , Phillips, E J P *Environ Sci Technol* **1992**, *26*, 2228
(9) Lovely D R Widman, J C , Woodward, J C Phillips, E J P *Appl Environ Microbiol* **1993**, *59*, 3572
(10) Shock E L Sassani, D C , Betz, H *Geochim Cosmochim Acta* **1997** *61* 4245
(11) Langmuir D *Aqueous Environmental Geochemistry*; Prentice Hall Inc Englewood Cliffs, NJ, 1997
(12) Albrechtsen, H J , Winding, A *Microb Ecol* **1992**, *23*, 303–317
(13) McLean R J C Fortin, D , Brown, D A *Can J Microbiol* **1996** *42* 392–400
(14) McCarthy J F , Zachara, J M *Environ Sci Technol* **1989**, *23*, 496–502
(15) Haas J R Bailey E H , Purvis O W *Am Mineral* **1998** *83*, 1494
(16) Macaskie L E , Empson, R M Cheetham A K Grey, C P , Skarnulis A J *Science* **1992**, *257*, 782
(17) Mann, H Fyfe, W S *Can J Earth Sci* **1985** *22* 1899
(18) Friis N Myers Keith P *Biotechnol Bioeng* **1986**, *28*, 21
(19) Cotoras, D Viedma, P Cifuentes, L , Mestre, A *Environ Technol* **1992**, *13*, 551
(20) Beveridge, T J , Murray, R G E *J Bacteriol* **1976**, *127*, 1502
(21) Beveridge, T J , Murray, R G E *J Bacteriol.* **1980**, *141*, 876
(22) Fein J B , Daughney, C J , Yee, N , Davis, T A *Geochim Cosmochim Acta* **1997**, *61*, 3319
(23) Daughney C J , Fein, J B *J Colloid Interface Sci* **1998**, *198*, 53
(24) Fowle, D A , Fein J B *Chem Geol* **2000** *168* 27–36
(25) Sakaguchi T *Abstracts of Euroconference on Bacteria-Metal/ Radionuclide Interaction Basic Research and Bioremdiation* **1998**, 7
(26) Stumm, W , Morgan, J J *Aquatic Chemistry*; Wiley New York, 1996
(27) Daughney C J , Fein, J B Yee N *Chem Geol* **1998**, *144*, 161
(28) Fowle, D A Fein J B *Geochim Cosmochim Acta* **1999**, *19/20*, 3059
(29) Fein, J B Delea, D *Chem Geol* **1999**, *161*, 373
(30) Sakaguchi T *Bioaccumulation of Uranium* Kyushu University Press Hukuoka, Japan, 1996 p 61
(31) Herbelin, A Westall J C *FITEQL 3 Report 94-01*, Department of Chemistry, Oregon State University Cornvallis, OR, 1994
(32) Wolery T J *EQ3NR UCRL-MA 110662 PT-III*, Lawerence Livermore National Laboratory Livermore, CA, 1992
(33) Andres Y , MacCordick J , Hurbert J C *FEMS Microbiol. Lett* **1994**, *115*, 27
(34) Martell A E , Smith, R M *Critical stability constants III Other organic ligands*; Plenum New York, 1977
(35) Martell A E Smith, R M *Critical stability constants V First supplement*; Plenum New York, 1982
(36) Langmuir, D *Chemical Modeling in Aqueous systems*, Jenne, E A. Ed American Chemical Society Washington, DC, 1979, p 353
(37) Helgeson H C Kirkham D H , Flowers G C *Am J Sci* **1981**, 281 1249
(38) Tripathi V S Ph D Dissertation Stanford University, Palo Alto, CA, 1983

Received for review December 8, 1999 Revised manuscript received May 16, 2000 Accepted June 7, 2000

ES991356H